Progress on the NML Trapped Ion Frequency Standards

Bruce Warrington, Peter Fisk, Malcolm Lawn and Michael Wouters

National Measurement Laboratory
CSIRO Telecommunications and Industrial Physics
PO Box 218, Lindfield NSW 2070
Sydney, Australia
Email: `bruce.warrington@tip.csiro.au`

Abstract

Microwave frequency standards based on the 12.6 GHz ground state hyperfine transition in trapped ^{171}Yb$^+$ ions have been under development at the CSIRO National Measurement Laboratory for several years. When the ions are cooled by a helium buffer gas, these standards have exceptional stability ($\sigma_y(\tau)$=5×10^{-14} $\tau^{-1/2}$) but are limited in absolute frequency accuracy to a few parts in 10^{13} by large second-order Doppler shifts. Laser-cooling the ions reduces these shifts, and significantly improves the accuracy without greatly degrading stability. We have also developed an all solid-state laser source to interrogate the ions in a buffer-gas cooled standard, which should allow continuous operation.

1. Introduction

The ability to confine, cool and manipulate atoms and ions using laser and electromagnetic techniques has led to remarkable improvements in the accuracy and stability of atomic frequency standards [1,2]. Confinement and cooling of atoms (and ions) makes it possible to use substantially extended atomic interrogation times and thereby decrease the measured spectral linewidth of the "*clock transition*" of the atoms. Furthermore, the resulting precise knowledge and control of the velocities, locations and trajectories of the atoms makes it possible to characterise very precisely the perturbations to the clock frequency caused by the atoms' environment [3].

The field of atomic microwave frequency standards based on cooling and trapping technology has evolved into two principal branches, one based on atoms and the other based on ions. Atom-based standards are mainly based on "fountain" technology, whereby the atoms (Cs or Rb) are launched into a free-fall trajectory during which the microwave interrogation takes place. Ion-based standards can use electromagnetic confinement to store the ions, bypassing the practical limit on the microwave interrogation time for earth-bound fountain devices, and allowing the clock transition to be resolved with much higher precision [4,5,6,7,8].

The performance trade-off between fountain and ion trap technologies currently appears to be between short term stability and accuracy. The short term stability of trapped ion microwave frequency standards benefits greatly from the very long microwave interaction times (1 minute or more [9,10,11]) which are possible. The accuracy and long term stability of trapped ion standards can be limited by our ability to calculate the effect of the confining electromagnetic fields on the frequency of the clock transition. However, work at NIST (discussed in more detail below) has demonstrated that trapped ion standards are capable of accuracies at least comparable to those of current Cs fountain standards, at the possible expense of short-term stability.

A small number of Cs fountain frequency standards are in, or about to commence, operation as primary laboratory frequency standards in national standards laboratories around the world.

Linear ion trap microwave frequency standards have been developed by the NASA Jet Propulsion Laboratory (JPL) to a level of maturity such that three are now operational as part of the NASA deep space tracking stations at Goldstone USA, Madrid Spain and Canberra Australia [12,13]. The work at JPL on linear ion trap microwave frequency standards has been oriented towards space science applications, with standards being developed and built to support deep space navigation, Very Long Baseline Interferometry and, more recently, compact designs for spacecraft. The JPL standards are based on the 40.5 GHz transition in the $^{199}Hg^+$ ion. Their outstanding short-term frequency stability, characterised by a fractional Allan deviation $\sigma_y(\tau) = 3\times10^{-14} \tau^{-1/2}$ [14] , arises principally from the good signal to noise ratio achievable by using large clouds of $\sim10^7$ ions cooled to around 500K through collisions with a helium buffer gas. These standards are not laser-cooled, and suffer from long term frequency drifts associated with the large second-order Doppler shifts resulting from the high ion temperature, the relatively large spatial extent of the ion cloud and inhomogeneity of the magnetic field over the ion cloud. Recent JPL ion trap designs have reduced some of these problems using the innovative technique of shuttling the ion cloud between one end of the trap where optical access is required for pumping and detection, and the other end, which incorporates better magnetic shielding, where the microwave interrogation is performed. A further innovation has been to use a 12-pole RF electrode geometry in the region of the trap where the microwave interrogation is performed. In such a 12-pole trap the field-free region along the axis of the trap is much larger than in a quadrupole trap of similar dimensions. Consequently, less motion is induced in a large cloud of ions by the trapping field, thereby reducing uncertainties and frequency instabilities which result from the second-order Doppler shift [15].

Also prominent amongst the recent work on linear ion trap microwave frequency standards is that undertaken at the National Institute of Standards and Technology (NIST). The standard at NIST is also based on the 40.5 GHz ground state hyperfine transition in the $^{199}Hg^+$ ion. Seven ions are confined in a linear Paul (RF) trap and laser-cooled to form a linear crystal along the nodal line of the RF electric field at the axial center of the trap. The walls of the ion trap vacuum enclosure are liquid helium cooled, eliminating ion loss and frequency shifts caused by collisions with background gas. By using Ramsey's method of separated fields to interrogate the clock transition with 100s between the $\pi/2$ pulses, a short-term frequency stability of $\sigma_y(\tau) = 3.3\times10^{-13} \tau^{-1/2}$ has been demonstrated. The frequency of the clock transition has been measured with a systematic uncertainty of 3.4 parts in 10^{15} which is comparable with accuracy values reported for Cs fountains. Furthermore, an improvement of at least one order of magnitude in the accuracy of this standard appears to be feasible [9].

The subject of the present paper is a microwave frequency standard based on buffer gas-cooled $^{171}Yb^+$ ions which has been under development at the CSIRO National Measurement Laboratory (NML) for several years. This system has demonstrated a short-term frequency stability of $\sigma_y(\tau)=5\times10^{-14} \tau^{-1/2}$ and its accuracy has been calculated as ±2 parts in 10^{13} [10,16]. The greatest contribution to the uncertainty is the second-order Doppler shift due to the thermal motion of the ions, which can in principle be made negligible by laser-cooling the ions to sub-Kelvin temperatures. However, it is necessary to perform the microwave interrogation with the cooling laser blocked to avoid a systematic light shift of the transition frequency. The interrogation takes several seconds, and during this period the ion cloud heats due to interaction with the confining RF fields and collisions with residual background gas. This heating sets an upper limit on the microwave interrogation time.

We have previously reported microwave spectroscopy on a laser-cooled cloud of approximately 10^4 $^{171}Yb^+$ ions with Ramsey pulse separations up to 10 s, where the cooling laser was blocked

throughout the interrogation sequence [11]. To our knowledge, the only other reported demonstration of microwave spectroscopy on laser-cooled ions with an interaction time of more than a few seconds (and where the cooling laser was blocked during this time) has been achieved by the NIST group where the ion trap is cooled to liquid helium temperatures [9]. The NML trap operates at room temperature.

Recent work has been devoted to measuring the temperature to which the ion cloud heats at the end of the interrogation, in order to evaluate the residual second-order Doppler shift and quantify the absolute frequency accuracy of the standard.

2. Experimental Apparatus

Details of the trapped ion frequency standards have been given previously [10] and are only summarised here. The ion cloud is confined in a linear Paul trap (Figure 1). Isotopically enriched ^{171}Yb is vaporised from a tantalum oven and ionised by electrons from a heated tantalum filament adjacent to the oven. The electron emission is confined to short pulses near a zero-crossing of the RF trapping field, in order to minimise buildup of stray charge near the trap. The trap is loaded with an RF amplitude of approximately 250 V_{pp} at 500 kHz and +5 V on the DC end electrodes. Both the RF and DC voltages are reduced for cooling, and the RF frequency is subsequently increased to 750 kHz at approximately 140 V_{pp}. The base pressure of the vacuum system is 4×10^{-8} Pa or better.

Figure 2 shows a partial energy-level diagram for Yb^{+}. There are three important transitions. The resonance transition near 369 nm is used for laser cooling, and to probe the populations of the ground state levels; this light is generated by a Coherent titanium-doped sapphire laser with an intracavity frequency doubling crystal. A small fraction of the ions decay to the metastable $^{2}D_{3/2}$ (F=1) level; the transition at 609 nm returns these ions to the cooling cycle, using light generated by a Spectra-Physics 380D dye laser. Finally, the transition between the ground state hyperfine levels is the reference frequency for the standard. Microwave radiation near 12 642 812 120 Hz for spectroscopy of this transition is synthesised from a signal generated by a sapphire-loaded superconducting dielectric resonator oscillator [17]. This radiation is also applied during cooling, in order to drain population accumulating in the lower hyperfine level.

Both the 369 nm and 609 nm beams are delivered to the ion trap using multimode optical fibres. The power of the 369 nm beam is actively stabilised using an acousto-optic modulator (AOM) at the fibre input. The 369 nm beam has a typical power of approximately 150 µW and a diameter of 1–2 mm, and the 609 nm beam a power of 10–20 mW and a diameter of 2–3 mm. Fluorescence at 369 nm is detected by a photon-counting photomultiplier tube (Hammamatsu R1332). A Newport UG11 filter is used to minimize noise from stray light. The photomultiplier signal is recorded using a Stanford Research SR400 photon counter and a PC-based data acquisition system. The PC also controls the frequency of the 369 nm laser, the trap loading sequence, the microwave frequency and amplitude, and laser beam shutters.

3. Measurement of Ion Temperature

We measure the temperature of the ion cloud by analysing the excitation spectrum, recorded as follows: the ion cloud is first cooled for a fixed interval with the laser frequency typically 20 MHz below line centre. The laser is then blocked for a time t, allowing the cloud to heat, and the frequency scanned to a new target frequency. The fluorescence recorded immediately after the

laser is unblocked is a measure of the amplitude of the emission spectrum at this frequency. The laser is then returned to the cooling frequency to cool the cloud for the next measurement. By varying the target frequency, the excitation spectrum is built up point by point.

The cloud is probably not in thermal equilibrium, and the concept of "temperature" should therefore be treated with some caution. It is nevertheless convenient to characterise the motional kinetic energy in a particular degree of freedom by an effective temperature. The measured temperature obtained from the width of the excitation spectrum thus characterises the kinetic energy of ion motion along the direction of the probe beam. Energy from the oscillating RF field can increase the kinetic energy of driven radial motion, equivalent to an increase in temperature. This increase may not couple immediately to the axial motion, depending on the rate of energy exchange between the motional degrees of freedom; equivalently, the temperatures characterising axial and transverse motion may differ. The other main heating mechanism, collisions with background gas, is isotropic and should heat axial and transverse motion equally.

3.1. Effective Temperature for Axial Motion

The axial case is simplest, as in this case ion micromotion due to the oscillating trap fields is negligible. A Voigt profile is fitted to the recorded spectrum by the method of least squares, and the Gaussian width is a direct measure of the temperature (see Figure 3). For short times the temperature is effectively too low to measure by this method; the lineshape analysis is not sufficiently sensitive to resolve a small Gaussian contribution to the Voigt profile. At longer times, it is apparent that the temperature can be maintained at or below 1 K for Ramsey interrogation times up to and beyond 10 s. To obtain these low temperatures, it is necessary to minimise the heating rate, in turn dependent on a number of factors including the background pressure, the size of the ion cloud, and the degree of heating due to RF micromotion. Work is continuing to identify these factors, to develop diagnostic measurements, and to establish methods of experimental control so that the temperature may be easily minimised (see for example §3.5).

3.2. Effective Temperature for Transverse Motion

For these measurements, the 369 nm beam is split into two components, an axial beam and a transverse beam of approximately 35 µW passing through the centre of the trap. Both beams are independently shuttered. The axial beam is used for cooling as before, and the transverse beam used only as a probe. A preliminary spectrum is shown in Figure 4.

Two principal difficulties complicate the transverse temperature measurement. The first is that the fluorescence signal obtained from the transverse probe beam is significantly smaller than the axial signal (by a factor of approximately 25) owing to the smaller spatial overlap with the cigar-shaped cloud, though the signal-to-noise ratio can be improved somewhat by aperturing the PMT to reduce background scatter. The second difficulty is that the lineshape is affected by the presence of radial ion micromotion, which introduces additional intrinsic broadening by adding sidebands spaced by multiples of the RF trap drive frequency to the normal Lorentzian component at line centre. A complete analysis is numerically complex, and to date has not been investigated. However, it is certainly true that the micromotion cannot *reduce* the width of the excitation spectrum. We can therefore set a preliminary upper limit on the transverse temperature by fitting a Voigt profile as for the axial spectra. The limit in this case is presently 2–3 K after two seconds, with no heating apparent during this interval. This fact, together with other experimental data,

supports the conclusion that the measured value gives an upper limit on the effective temperature of the transverse motion.

3.3. Frequency Scale Calibration

Although it is possible in principle to scan the probe laser frequency using the AOM, in which case the frequency shift is readily calibrated, we do not have a modulator with sufficient frequency scan range to record the entire profile. The laser frequency is set by the control electronics of the Ti:Sapphire laser, and must consequently be separately calibrated.

Such a calibration would typically refer to either an etalon with a calibrated free spectral range or the known isotopic and hyperfine structure of the resonance transition itself. However, both these methods would require a scan width of many GHz, since this is the typical component separation in the reference scale. To establish a frequency calibration on the scale of the lineshape scan width (of order 200 MHz), two separate orders of the AOM output were focussed into the optical fibre carrying the 369 nm light to the trap. A recorded excitation spectrum consequently shows two peaks separated by the AOM drive frequency (Figure 5), which can be directly measured.

3.4. Systematic Effects

We have investigated a number of systematic effects which can perturb the recorded excitation spectrum. Two of the most significant are discussed here. Firstly, as noted above, the frequency of the probe beam is not scanned using an AOM but is set by the control electronics of the Ti:Sapphire laser. As the spectrum is recorded, the laser frequency is scanned first to one side of the cooling frequency and then the other, returning to the cooling frequency between each point. Any hysteresis in the laser frequency scan will therefore introduce a systematic distortion in the recorded profile. Hysteresis is usually present at some level in ring lasers of the type used here, due to mechanical hysteresis in galvanometers used to vary the optical cavity length. Careful investigation confirms that the effects of hysteresis can be avoided if each target frequency is always approached from the same side, for example by always scanning the laser to the lower limit of the scan range before returning to the appropriate target frequency.

Secondly, the interaction between the resonant probe light and the ion cloud can perturb the ion temperature during the probe interval. The perturbation is asymmetric about line centre: the profile amplitude is increased at low frequencies as the cloud is cooled, and reduced at high frequencies as the cloud heats. The extent of the perturbation can be investigated by recording the excitation spectrum as a function of time after the probe light is applied, by appropriate gating of the photon counter at each frequency point, and the asymmetry can be detected by fitting a theoretical profile which allows two different temperatures below and above line centre (see for example Figure 6). To minimise distortion, the probe interval is selected to be as short as possible. The power in the 369 nm beam is usually reduced during the probe interval, by reducing the amplitude of the drive to the intensity stabilisation AOM, and restored for laser cooling.

3.5. Ion Micromotion

The amplitude of ion micromotion is a significant factor in the heating rate for the laser-cooled ion cloud. It is apparent that micromotion at the RF trap drive frequency Ω modulates the fluorescence light at this frequency; we resolve this modulation by gating a photon counter synchronously with the trap drive. The amplitude of the modulation can then be used as a diagnostic to assist in minimising the micromotion. Time-resolved fluorescence data recorded for

both the axial and transverse beams are shown in Figure 7. The spectral content of the modulation can also be used, in principle, to obtain more detailed information about the micromotion, but this has not yet been investigated.

4. Solid-state Laser Sources

At present, the 369 nm resonance light is generated using a Ti:Sapphire laser pumped by a high-power Ar^+ gas laser. Long-term operation of the trapped Yb^+ frequency standards requires a laser which needs no maintenance and which is cheap to run. We have therefore built a compact solid-state source based on frequency doubling of a grating-stabilised diode laser at 739 nm. The system is based on the Sharp LT031MD0 diode; the nominal centre wavelength of this diode is 750 nm, so that the entire laser cavity must be cooled to –40 °C for operation at 739 nm. The diode laser output is externally doubled using a $LiIO_3$ crystal in a resonant cavity with a power enhancement of about 400. The narrow linewidth of the cavity means that the coupling to the cavity, and therefore the cavity output power, depends principally on the laser linewidth. The laser must usually be very carefully adjusted to minimise its linewidth. With an input power at the cavity of 5 mW, about 25 µW at 369 nm is readily obtained and under optimal conditions up to 40 µW has been obtained. At present, the passive stability of the laser is such that it will operate for about two weeks before mode hopping.

The output power and short term frequency stability of this laser (±10 MHz over a period of 10 s) are at present not sufficient to enable laser cooling of the relatively large ion cloud confined by the current traps. However, the power is sufficient to serve as a probe for a buffer-gas cooled standard, and should provide continuous operation with minimal maintenance. In the future, it is possible that an improvement in either the power available at 739 nm (by using a different diode) or in the efficiency of frequency doubling (by using a periodically-poled doubling crystal) may allow the laser to be used also for laser cooling.

5. Conclusion

The maximum achievable stability for a frequency standard based on laser-cooled $^{171}Yb^+$ ions is predicted to be better than $\sigma_y(\tau) = 5\times10^{-14}\ \tau^{-1/2}$, which is comparable to the NML buffer-gas cooled standard. This prediction assumes a cloud of radius 1 mm and length 10 mm containing approximately 10^4 ions, a Ramsey pulse separation of 10 s, and a cycle time of 13 s after allowing for cooling periods. Estimates of the dominant systematic frequency offsets are given in Table 1 (reproduced from Ref. [16]), with a combined estimate of the absolute fractional frequency uncertainty of approximately 4×10^{-15}. Based on these estimates, a cloud of laser-cooled $^{171}Yb^+$ ions in a linear trap continues to show significant promise as a frequency standard of high accuracy and stability.

References

[1]   Bergquist, J.C. ed*., Proc. of the 5th Symposium on Frequency Standards and Metrology*, World Scientific Singapore, 1996.

[2]   Major, F. G., *"The Quantum Beat"*, Springer-Verlag New York Inc., 1998.

[3]   Fisk, P. T. H., 1997, *Rep. Prog. Phys.* **60**, 761-817.

[4]   Clairon, A., Ghezali, S., Santarelli, G., Laurant, Ph., Lea, S. N., Bahoura, M., Simon, E., Weyers, S., and Symaniec, K., in reference [1], 49-59.

[5]   Jefferts, S. R., Meekhof, D. M., Shirley, J. H., and Parker, T. E., 1999, *Proc. 1999 Joint Meeting EFTF and IEEE FCS*, IEEE **99CH36313**, 12-15.

 [6] Weyers, S., Bauch, A., Griebsch, D., Hübner, U., Schröder, R., and Tamm, Ch., 1999, *Proc. 1999 Joint Meeting EFTF and IEEE FCS*, IEEE **99CH36313**, 16-19.

[7]   Swanson, T. B., Burt, E. A., and Ekstrom, C. R., 2000, *Proc. 2000 IEEE FCS,* IEEE **00CH37052**, 672-675.

[8]   Fertig, C., Bouttierm, J. and Gibble, K., 2000, *Proc. 2000 IEEE FCS*, IEEE **00CH37052**, 680-686.

[9]   Berkeland, D. J., Miller, J. D., Bergquist, J. C., Itano, W. M. and Wineland, D. J., 1998, *Phys. Rev. Lett.*, **80**, 2089–2092.

[10] Fisk, P. T. H., Sellars, M. J., Lawn, M. A. and Coles, C., 1997, *IEEE Trans. Ultrasonics, Ferroelectrics and Frequency Control*, **44**, 344–354.

[11] Warrington, R. B., Fisk, P. T. H., Wouters, M. J., Lawn, M. A. and Coles, C., 1999, *Proc. 1999 Joint Meeting EFTF and IEEE FCS*, IEEE **99CH36313**, 125–128.

[12] Tjoelker, R. L., Bricker, C., Diener, W., Hammel, R. L., Kirk, A., Kuhnle P., Maleki, L., Prestage, J. D., Santiago, D., Seidel, D., Stowers, D. A., Sydnor, R. L. and Tucker, T., 1996, *Proc. 1996 IEEE FCS*, IEEE **96CH35935**,1073–1081.

[13] Tjoelker, R. J., *personal communication*.

[14] Prestage, J. D., Tjoelker, R. L., and Maleki, L., 1999, *Proc. 1999 Joint Meeting EFTF and IEEE FCS*, IEEE **99CH36313**, 121-124.

[15] Prestage, J. D., Tjoelker, R. L., and Maleki, L., 2000, *Proc. 2000 IEEE FCS*, IEEE **00CH37052**,706-710.

[16] Fisk, P. T. H., Lawn, M. A. and Coles, C., 1997, *Proc. Workshop on the Scientific Applications of Clocks in Space*, NASA Jet Propulsion Laboratory Publication **97-15**, 143-152.

[17] Giles, A. J., Mann, A. G., Jones, S. K., Blair, D. G. and Buckingham, M. J., 1990, *Physica B*, **165-166**, 145.
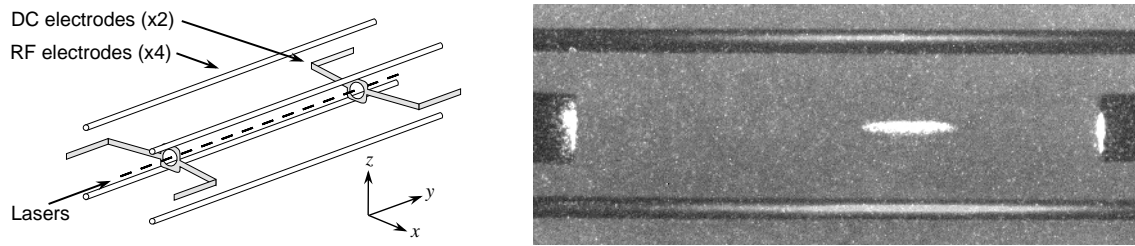
Figure 1: (Left) Electrode configuration of the linear trap. We refer to motion in the *y* direction as axial, and in the *x-z* plane as transverse. (Right) The laser-cooled ion cloud, approximately 10 mm long with a radius of 1.5 mm. RF electrodes are visible top and bottom (diameter 2.3 mm, separation 20 mm) and DC electrodes left and right (separation 60 mm).
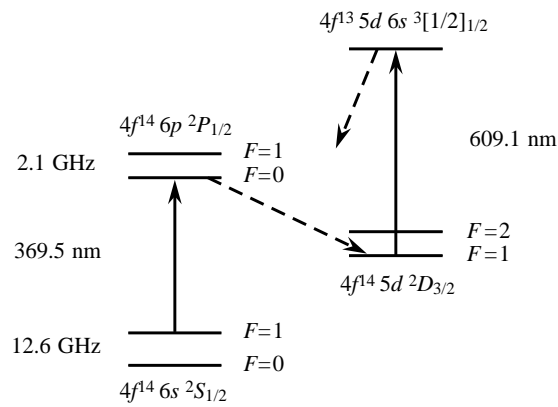

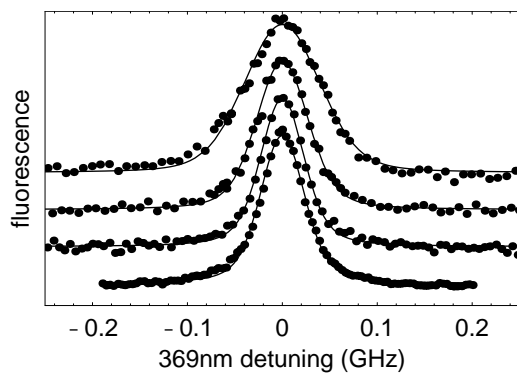Figure 2: Partial energy level diagram of the ^{171}Yb$^+$ ion.

Figure 3: Axial excitation spectra. Reading upwards from the lowest trace, t=5 s and T=1 K; 10 s, 1 K; 15 s, 1.5 K; 20 s, 3.5 K.

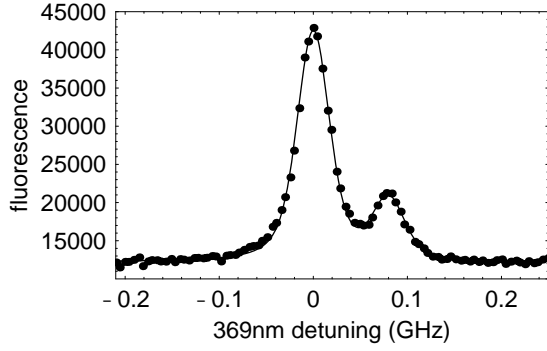Figure 4: Transverse (upper) and axial (lower) excitation spectra recorded under the same conditions.

Figure 5: Calibration of the frequency scale, using an acousto-optic modulator to generate two frequencies separated by a known interval (80 MHz).
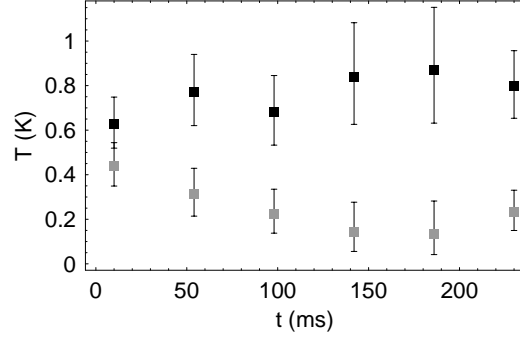

Figure 6: Upper and lower traces show temperature T obtained from half-profiles above and below line centre varying with time t after shutter opens.
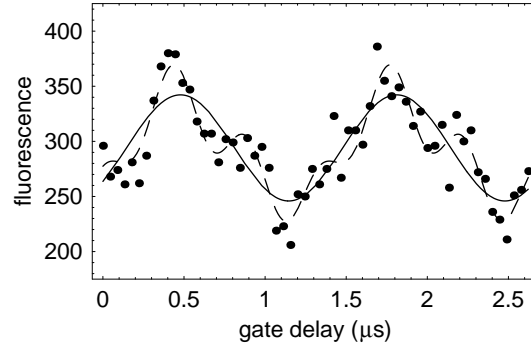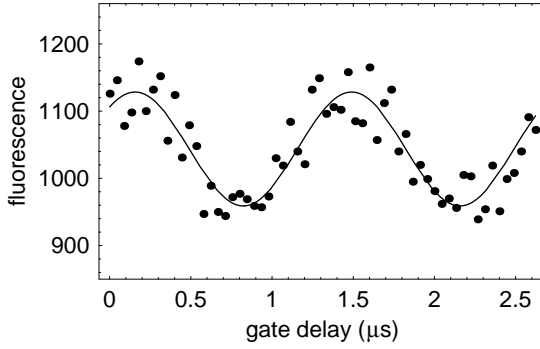

Figure 7: Time-resolved fluorescence for the axial (left) and transverse (right) probe beams, modulated at the trap frequency of 750 kHz; higher harmonics are also visible in the transverse signal. The modulation is used as a diagnostic to minimise heating due to ion micromotion.

Shift	Magnitude	Uncertainty
Second-order Doppler	5×10^{-15}	2×10^{-15}
Second-order Zeeman	3×10^{-13}	2×10^{-15}
AC Zeeman	$<2 \times 10^{-15}$	1×10^{-15}
Blackbody shift	2×10^{-14}	1×10^{-15}
Microwave non-ideality	1×10^{-15}	1×10^{-15}

Table 1: Estimates of the dominant offsets to the frequency of the clock transition and their uncertainties.